Table 2 Rotation-induced pulse tilt angle and time delay for two values of θ_s and $r_e = R', 2R', 3R'$ considered for PSR1937+214

r_e	θ_s (deg)	Tilt angle (deg)	Time delay for δ (μs) ±1°	±2°	±3°	±4°	±5°
R'	54	10.262	0.2	0.5	0.7	1.0	1.2
	90	10.253	0.3	0.6	1.0	1.3	1.5
$2R'$	54	20.199	0.8	1.6	2.4	3.1	3.9
	90	20.322	1.0	1.9	2.8	3.9	4.7
$3R'$	54	28.823	1.5	3.1	4.6	6.1	7.7
	90	29.290	1.8	3.6	5.4	7.2	9.1

proportional to δ. This is also evident in ε'. Figure 2 illustrates (for $\delta = 0°, \pm 5°$) the variation $\varepsilon'(r_e)$, r_e being taken in units of $R'(R)$ which is the radius of the rotating (non-rotating) neutron star.

One interesting result of our calculations is the 'sweeping' of the entire pulse cone in the direction of rotation of the pulsar, thus imparting a tilt to the cone. The tilt can be understood in terms of the net bending of the radially outward $\delta = 0$ photon, whose values for various θ_s and r_e are given in Table 2.

In Schwarzchild space-time, photons emitted at $\pm\delta$ would have the same time of flight to the distant observer. But with the neutron star rotating rapidly, this symmetry will not be maintained. The backward emitted photons would have larger time of flight than the forward emitted photons. The difference in the arrival times of $\pm\delta$ photons, which we call time delay, can be evaluated from the equations of motion of photons in the external space-time and their redshifts. These values are listed in Table 2. If the time delay between photons with maximum δ and minimum δ equals the pulse duration, the complete pulse will be detected by the observer. If, however, this time delay exceeds the pulse duration, then, photons with δ larger than a critical δ will miss the detector. As a result, the pulse will have a gradual buildup but a steeper falloff. This will be a contributory factor to the asymmetry in the final pulse profile (apart from the effects resulting from inertial frame drag and interstellar/planetary scintillation, if any), and, in principle, will constrain the duty cycle of the pulsar.

The effects of curvature and rotation on the pulse profile presented here are purely general relativistic effects, and will be additional to any (frequency dependent) effect on the propagation of electromagnetic waves through anisotropic/inhomogeneous magnetized plasma. Observationally, most pulsars show narrow profiles. Our calculations, therefore, can be taken to imply that at the emission location, the pulse starts out in the shape of a narrow spike. As the brightness temperature of the source is directly proportional to the intensity of radiation, the important conclusion that follows is that the brightness temperatures of pulsars in general (since the curvature effects are dominant over the rotational effects) are larger by an order of magnitude (in the emitter's frame of reference) than are presently presumed.

We thank Professors J. V. Narlikar, Ch. V. Sastry, V. Radhakrishnan and our colleagues at the Raman Research Institute, for helpful discussions. B.D. acknowledges the Indian National Science Academy for the award of Biren Roy Trust Fellowship.

Received 12 February; accepted 2 April 1985.

1. Backer, D. C., Kulkarni, S. R., Heiles, C., Davis, M. M. & Goss, W. M. *Nature* **300**, 615-618 (1982).
2. Boriakoff, V., Buccheri, R. & Fauci, F. *Nature* **304**, 417-419 (1983).
3. Harding, A. K. *Nature* **303**, 683-684 (1983).
4. Shapiro, S. L., Teukolsky, S. A. & Wasserman, I. *Astrophys. J.* **272**, 702-707 (1983).
5. Datta, B. & Ray, A. *Mon. Not. R. astr. Soc.* **204**, 75p-80p (1983).
6. Ray, A. & Datta, B. *Astrophys. J.* **282**, 542-549 (1984).
7. Friedman, J. L. *Phys. Rev. Lett.* **51**, 11-14 (1983).
8. Friedman, J. L., Ipser, J. R. & Parker, L. *Nature* **312**, 255-257 (1984).
9. Arons, J. *Nature* **302**, 301-305 (1983).
10. Ray, A. & Chitre, S. M. *Nature* **303**, 409-410 (1983).
11. Kapoor, R. C. & Datta, B. *Mon. Not. R. astr. Soc.* **209**, 895-904 (1984).
12. Hartle, J. B. & Thorne, K. S. *Astrophys. J.* **153**, 807-834 (1968).
13. Thorne, K. S. *General Relativity and Cosmology* (ed. Sachs, R. K.) 237 (Academic, New York, 1971).
14. Misner, C. W., Thorne, K. S. & Wheeler, J. A. *Gravitation* (Freeman, San Francisco, 1973).
15. Radhakrishnan, V. & Cooke, D. J. *Astrophys. Lett.* **3**, 225-229 (1969).

Possible precipitation of ice at low latitudes of Mars during periods of high obliquity

Bruce M. Jakosky

Laboratory for Atmospheric and Space Physics, University of Colorado, Boulder, Colorado 80309, USA

Michael H. Carr

US Geological Survey, Menlo Park, California 94025, USA

Most of the old cratered highlands of Mars are dissected by branching river valleys that appear to have been cut by running water[1,2] yet liquid water is unstable everywhere on the martian surface. In the equatorial region, where most of the valleys are observed, even ice is unstable[3,4]. It has been suggested, therefore, that Mars had an early denser atmosphere with sufficient greenhouse warming to allow the existence of liquid water[5]. Here, we suggest instead that during periods of very high obliquities, ice could accumulate at low latitudes as a result of sustained sublimation of ice from the poles and transport of the water vapour equatorwards. At low latitudes, the water vapour would saturate the atmosphere and condense onto the surface where it would accumulate until lower obliquities prevailed. The mechanism is efficient only at the very high obliquities that occurred before formation of Tharsis very early in the planet's history, but limited equatorial ice accumulation could also have occurred at the highest obliquities during the rest of the planet's history. Partial melting of the ice could have provided runoff to form the channels or replenish the groundwater system.

That some mechanism must exist for replenishment of the equatorial inventory of water has been suspected on several grounds: (1) if the valleys formed in a manner analogous to terrestrial river valleys, by slow erosion of running water, then the volumes of water that would have flowed through them would have been so large that some recycling of water is implied; (2) although groundwater seepage has probably had a major role in formation of the valleys[6], several morphological characteristics suggest that precipitation was also involved, so that transfer of water from the atmosphere to the surface occurred[2]; (3) the unique characteristics of several martian landforms, particularly those formed by impact, have been attributed (although not uniquely) to the presence of ground ice in regions where it is unstable.

We have calculated the potential loss of water from the poles on the assumption that sublimation of the seasonal CO_2 cap during summer exposes a residual water-ice cap, as is currently the case for the North Pole[7,8] and may occasionally be the case for the South Pole[9]. The procedure followed here is similar to that used by Toon *et al.*[10]. Temperatures at the surface and down to depths of 7 m are calculated for ±85° lat. taking into account incident solar radiation, long-wave emission from the surface and atmosphere, conduction into the ground, sublimation and condensation of carbon dioxide and evaporation of water. Atmospheric pressures greater than the present value may occur at high obliquities as a result of desorption of CO_2 from the high-latitude regolith[11]. We assumed that the pressure was 40 mbar at 45° obliquity, 25 mbar at 35° obliquity and 10 mbar at the current 25° obliquity[12]. The main difference between our model and that of Toon *et al.* is that we included growth and decay of the CO_2 cap as an integral part of our model rather than assuming that the CO_2 cap disappeared at a specific time. Our results are conservative in that they give estimates of the

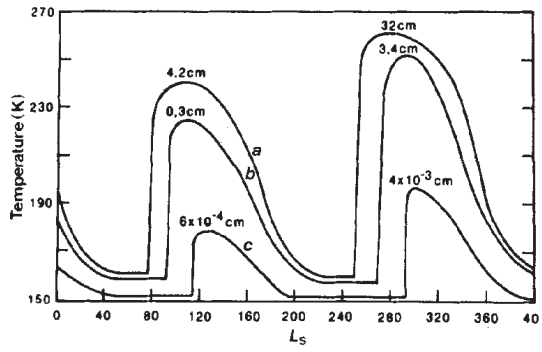

Fig. 1 Seasonal polar cap temperatures calculated for obliquities of 45° (*a*), 35° (*b*) and 25° (*c*). The adjacent numbers refer to the thickness of ice sublimed from the cap (in cm) during the entire summer. For clarity, only temperatures for the warmer pole are shown at each season. Calculations assume the maximum obliquity (0.14) and have periapsis at southern solstice, and thus yield the maximum differences between the two poles; other choices would yield temperatures intermediate between these extremes.

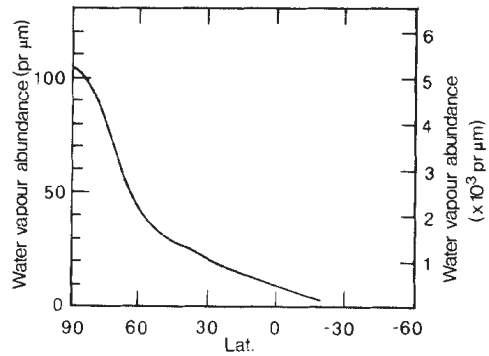

Fig. 2 Latitudinal distribution of water vapour at mid-summer in the north as observed from the Viking space craft (left-hand ordinate). The right-hand ordinate is appropriate for high values for the obliquity, when $\geq 5\times10^3$ pr μm water may be present over the cap.

amount of water sublimed from the summer cap that are up to a factor of 10 lower than the estimates of Toon *et al.*[10].

Typical results are shown in Fig. 1 for the three values of the obliquity. Although the results are sensitive to factors such as the albedo of CO_2 and water frost, the wind speed and the assumed thermal conductivity, the results, in general, demonstrate that at 45° obliquity a few centimetres to a few tens of centimetres will be evaporated from the poles during each summer. At an obliquity of 35° a few tenths of a centimetre to a few centimetres will be lost, while in present conditions only 10^{-2}–10^{-4} cm are lost.

The results shown in Fig. 1 were calculated assuming sublimation of water into a dry atmosphere. The actual amount of water sublimed and its eventual fate will depend on the rate of atmospheric transport away from the pole. Figure 2 shows the mid-northern-summer latitudinal distribution of water vapour during 1976. Polar abundances of about 100 precipitable (pr) μm were observed, consistent with an almost saturated atmosphere[8,13]. Non-polar atomospheric water indicates transport of water away from the pole and/or exchange of water between the regolith and atmosphere[14,15], although transport from the poles ultimately dominates the process[15]. For equatorial and mid-latitude mixing timescales indicated by dynamic models[16,17], an amount of the order of 5×10^{14} g H_2O can be transported southwards each year, equivalent to removing $\sim4\times10^{-2}$ g cm^{-2} from the cap[15,18]. Given the uncertainties in the models, this value is consistent with the estimated amounts of water that can be sublimed.

At high obliquity, a similar atmospheric circulation pattern should exist, with the exceptions of a poleward shift in the Hadley cell to the subsolar point, and more vigorous cross-equatorial transport (ref. 19 and R. M. Haberle, personal communication). Therefore, if we assume a similar mid-summer distribution of water with latitude due to transport from the polar region, we can use Fig. 2 to show the latitudinal variation at midsummer, reading now from the right-hand scale. The estimate of 5×10^3 pr μm over the pole is conservative, based on saturation of the atmosphere over the pole at temperatures that are relatively low for 45° obliquity but higher than that of the present summer cap. By scaling the amount transported to the total abundance, the amount of water transported away from the cap is equivalent to removal of ~2 g cm^{-2} from the pole, again consistent with the amounts estimated to have sublimed. From the right-hand scale of Fig. 2, there can be >1,000 pr μm of atmospheric water at mid- and low latitudes. For less conservative assumptions, the amount of water ice sublimed can be as great as 20 cm and the water content of the atmosphere at the equator can be as high as 10,000 pr μm.

At the equator a dust-free atmosphere is capable of holding only as much as 100–200 pr μm of water vapour without saturating[20,21]. Thus, the excess above this value will condense and form clouds. Persistent dust storms are, however, likely at high obliquities[5]. The presence of dust causes atmospheric temperatures to rise. As a result, the atmosphere could hold 5,000–10,000 pr μm during the day without saturating, and up to 300 pr μm at night[21]. Thus, even during dust storms water would condense out at night if abundances were higher than ~300 pr μm. If the dust acts as condensation nuclei for the water, then the dust and ice will be removed rapidly to the surface, possibly within several days. Two uncertainties are the effect of the ice clouds on the holding capacity of the atmosphere and the effect of surface ice. Temperatures that occur in the presence of clouds are not well determined; low-altitude clouds will cool the surface dramatically[22,23] while high-altitude clouds could increase surface temperatures[10]. The presence of high-albedo ice on the surface would significantly lower surface and atmospheric temperatures, thereby providing a positive feedback and enhancing the tendency for atmospheric water to condense.

If as much as 20 cm of ice are removed in 1 yr from the summer cap and deposited uniformly between ±45° latitude, the resulting ice thickness is 0.4 cm. It is uncertain, however, where the ice is deposited. The atmospheric circulation pattern and the relative timescales for condensation and settling will determine whether the ice is deposited near the edge of the summer or winter cap or more uniformly over the globe. During the following winter, the non-polar water vapour abundance at saturation will not change significantly, while the winter polar cap will have essentially no water vapour above it. The latitudinal gradient of water during winter is thus towards the pole, but is a factor of 5–50 smaller in magnitude than during summer, so that the rate of transport of water from low latitudes to the winter pole is probably low. Also, at the time when water is seeking to move back to the winter pole, additional water is being supplied from the other summer pole, further inhibiting evaporation. Ice will thus tend to accumulate in non-polar regions.

The thickness of ice that could accumulate at low latitudes and the fraction of the obliquity cycle during which it would be stable depends on the amount of ice available at the poles and the range of the obliquity variations. Before the formation of Tharsis the mean obliquity was as high as 35° and the peak value as high as 45° (ref. 24). During the highest obliquities of this epoch, 2 km of ice could be removed from the poles in $<10^4$ yr to form ice deposits tens of metres thick in the non-polar latitudes, if that much polar ice is available. Ice may have returned to the poles only at minimum obliquities. During most of Mars' history, however, obliquities ranged from 15 to 35° (refs 24, 25). Net accumulation of ice in non-polar areas is then likely only at peaks in the obliquity cycle, and removal of as much as 2 km of ice from the poles is unlikely. The polar layered deposits could, however, be extensively reworked, as is suggested by the scarcity of superimposed impact craters[5,10].

Meltwater from the ice deposits may have contributed to the erosion of the branched valley networks. For melting temperatures to be reached at the surface by greenhouse warming, atmospheric pressures near 1 bar are required[26]. However, melting of snow or ice does not necessarily require surface temperatures to be above melting. The low thermal conductivity of snow and its partial transparency to sunlight can result in subsurface melting when surface temperatures are well below freezing[27]. Thus, melting can occur in substantially thinner atmospheres than are required by the atmospheric greenhouse effect alone. Another appealing reason to invoke a mechanism that requires high obliquities to explain the valley networks is that most of the networks formed very early in Mars' history[2,28]. At that time, the Tharsis bulge may not have reached its present size. As Tharsis grew, the maximum obliquities reached decreased, and as a result so did the efficacy of the equatorward transfer of water. Young valley networks are, therefore, rare.

We thank R. W. Zurek, R. T. Clancy, R. M. Haberle, O. B. Toon and F. D. Palluconi for useful discussions. This work was supported by NASA grant NAGW-552 at the University of Colorado and by NASA work order W25,462 at the US Geological Survey.

Received 17 December 1984; accepted 10 April 1985.

1. Baker, V. R. *The Channels of Mars* (University of Texas Press, 1982).
2. Carr, M. H. *The Surface of Mars* (Yale University Press, 1981).
3. Fanale, F. P. *Icarus* **28**, 179-202 (1976)
4. Farmer, C. B. & Doms, P. E. *J. geophys. Res.* **84**, 2881-2888 (1979).
5. Pollack, J. B. & Toon, O. B. *Icarus* **50**, 259-287 (1982).
6. Pieri, D. C. *Science* **210**, 895-897 (1980).
7. Kieffer, H. H., Chase, S. C. Jr, Martin, T. Z., Miner, E. D. & Palluconi, F. D. *Science* **194**, 1341-1344 (1976).
8. Farmer, D. B., Davies, D. W. & Laporte, D. D. *Science* **194**, 1339-1341 (1976).
9. Jakosky, B. M. & Barker, E. S. *Icarus* **57**, 322-334 (1984).
10. Toon, O. B., Pollack, J. B., Ward, W., Burns, J. A. & Bilski, K. *Icarus* **44**, 552-607 (1980).
11. Fanale, F. P. & Cannon, W. A. *J. geophys. Res.* **79**, 3397-3402 (1974).
12. Fanale, F. P., Salvail, J. R., Banerdt, W. B. & Saunders, R. S. *Icarus* **50**, 381-407 (1982).
13. Davies, D. W. *J. geophys. Res.* **87**, 10253-10263 (1982).
14. Jakosky, B. M. *Icarus* **55**, 1-18 (1983).
15. Jakosky, B. M. *Icarus* **55**, 19-39 (1983).
16. Haberle, R. M. Leovy, C. B. & Pollack, J. B. *Icarus* **50**, 322-378 (1982).
17. Pollack, J. B., Leovy, C. B., Greiman, P. W. & Mintz, Y. *J. atmos. Sci.* **38**, 3-29 (1981).
18. Jakosky, B. M. & Farmer, C. B. *J. geophys. Res.* **87**, 2999-3019 (1982).
19. Haberle, R. M. *Pap. Div. planet. Sci.*, Boulder (1982).
20. Davies, D. W. *J. geophys. Res.* **84**, 8335-8340 (1979).
21. Jakosky, B. M. *Space Sci. Rev.* (in the press).
22. Rossow, W. B., Henderson-Sellers, A. & Weinreich, S. K. *Science* **217**, 1245-1247 (1982).
23. Twomey, S. *Atmospheric Aerosols* (Elsevier, New York, 1977).
24. Ward, W. R., Burns, J. A. & Toon, O. B. *J. geophys. Res.* **84**, 243-259 (1979).
25. Ward, W. R. *J. geophys. Res.* **84**, 237-241 (1979).
26. Hoffert, M. I., Calligari, A. J., Hsieh, C. T. & Ziegler, W. *Icarus* **47**, 112-129 (1981).
27. Clow, G. D. in *Workshop on Water on Mars*, 15-16 (Lunar Planetary Institute, Houston, 1984).
28. Carr, M. H. & Clow, G. D. *Icarus* **48**, 91-117 (1981).

Onset of the south-west monsoon and sea-surface temperature anomalies in the Arabian Sea

R. Kershaw

Meteorological Office, Bracknell, Berkshire RG12 2SZ, UK

In 1979, the year of the Global Weather Experiment, the atmosphere and ocean of the monsoon region were particularly well observed. For this reason, the onset period of the monsoon, 11–19 June 1979, was selected for international comparison of numerical prediction models[1]. Previous studies[2–4] have demonstrated that successful predictions for this period are difficult to achieve. I report here two examples of numerical predictions that highlight the role of sea-surface temperatures, namely a control forecast using climatological sea-surface temperatures and an anomaly forecast using more realistic (and warmer) surface temperatures specified for the eastern Arabian Sea. It is shown that the use of the more accurate sea-surface temperatures enables a better prediction of the development of a monsoon depression to be obtained.

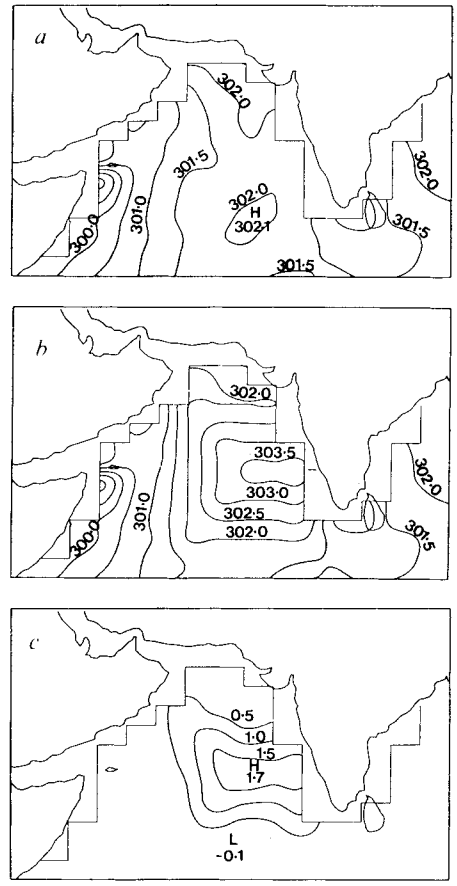

Fig. 1 *a*, Sea-surface temperature for control forecast; *b*, sea-surface temperature for anomaly forecast; *c*, sea-surface temperature anomaly ($b - a$). Contour interval, 0.5 K.

For these experiments, the 11-layer global atmospheric general circulation model[5,6] of the UK Meteorological Office was used with a horizontal resolution of 2° lat. and 3° long. The initial conditions for both forecasts were taken from the (level 3B) analysis for 12.00 GMT on 11 June 1979 made by the European Centre for Medium Range Weather Forecasts (ECMWF) using data which had been collected for the Global Weather Experiment. The sea-surface temperatures were fixed throughout the 8 days of each forecast. The values in Fig. 1*a* were derived from a climatological average for the decade 1951–60; those for the eastern Arabian Sea in Fig. 1*b* were based on an analysis by Seetaramayya and Master[7] for 8–15 June 1979. The difference chart (Fig. 1*c*) shows a maximum warm anomaly of 1.7 K in this region.

The onset of the monsoon is characterized by an increase in wind speeds at low levels over the Arabian Sea and the commencement of the rains along the west coast of India. Figure 2*a*, *b* illustrates the changes in the wind field at the 850-mbar pressure level during the onset period. On 11 June the south-westerly jet had a maximum speed of 14 m s^{-1} a few degrees to the east of the Somali peninsula, and the main branch of the monsoon flow was still to the south of India (Fig. 2*a*). During the next 8 days the jet strengthened and extended eastwards to the southern tip of India. A depression formed on the northern flank of the jet and moved first north then west, allowing the monsoon westerlies to advance northwards to cover much of the Indian peninsula and bring the rains to the west coast. By 19 June the maximum speed of the jet was 29 m s^{-1} and the cyclonic vortex of the depression was near the Arabian coast (Fig. 2*b*).

In the control forecast, the jet strengthened and extended eastwards more slowly than actually occurred, to give a maximum speed of only 24 m s^{-1} by 19 June (Fig. 2*c*). A weak vortex developed in the correct location, but the model failed to intensify it and kept it stationary. The anomaly run produced